J Mater Sci (2018) 53:4961–4973

Composites

One-pot synthesis of Mn_3O_4/graphitic carbon nanoparticles for simultaneous nanomolar detection of Pb(II), Cd(II) and Hg(II)

Prashanth Shivappa Adarakatti[1,2], Vijaya Kumar Gangaiah[1], Craig E. Banks[3], and Ashoka Siddaramanna[4,*]

[1] Department of Chemistry, Central College Campus, Bangalore University, Bengaluru, India
[2] Present address: Solid State and Structural Chemistry Unit, Indian Institute of Science, Bengaluru, India
[3] Faculty of Science and Engineering, Manchester Metropolitan University, Chester Street, Manchester M1 5GD, UK
[4] Department of Chemistry, School of Engineering, Dayananda Sagar University, Kudlu Gate, Bengaluru, India

Received: 25 August 2017
Accepted: 6 December 2017
Published online: 27 December 2017

ABSTRACT

In this paper, a facile one-step sucrose–nitrate decomposition method has been proposed to synthesis Mn_3O_4 nanoparticles (Mns)/graphitic carbon. The prepared material has been characterized by X-ray diffraction, Fourier transform infrared spectrometer, surface area analysis and transmission electron microscopy. The prepared Mns/graphitic carbon is drop-casted on glassy carbon electrode to allow the fabrication of electrochemical sensors for the simultaneous detection of Pb(II), Cd(II) and Hg(II) at nanomolar (nM) levels in aqueous solutions via differential pulse anodic stripping voltammetry. The proposed Mns/graphitic carbon sensors exhibit a wide linear range from 20 to 680 nM towards the simultaneous sensing of Cd(II), Pb(II) and Hg(II), and the corresponding limits of detection were found to be 0.48×10^{-11}, 9.66×10^{-11} and 0.51×10^{-11} M, respectively. The practical application of the proposed sensor is evaluated within a real battery, industrial and chrome plating effluents.

Introduction

Pb(II), Cd(II) and Hg(II) are highly toxic heavy metal ions (HMIs), and the discharge of these ions into the environment is conspicuously increasing due to the various industrial activities such as metallurgical, paint and fertilizer industries [1, 2]. Severe toxicity and exposure to these metal ions even at trace-level concentrations cause the effects on both mankind and aquatic systems in the form of adverse health effects such as neurological damage, hindered growth, anaemia, kidneys and hypertension [3]. Consequently, the World Health Organization (WHO) has recommended the maximum threshold limit value in drinking water for Pb(II), Cd(II) and Hg(II) be 10, 3 and 1 nM, respectively [4]. Hence, the measurement of these toxic ions at trace-level concentrations is of great importance for governmental and non-

Address correspondence to E-mail: ashok022@gmail.com

https://doi.org/10.1007/s10853-017-1896-6

governmental agencies to control the levels of these pollutants.

In order to measure and monitor the levels of these pollutants, several protocols have been developed for the quantification of Pb(II), Cd(II) and Hg(II) ions using various spectroscopic methods [5–9]. The reported spectroscopic methods require sophisticated instruments, prolonged sample preparation, careful handling along with skilled personnel to perform the trial and more importantly not preferable for field analysis.

An alternative to the above-mentioned approaches is the use of electrochemical technology which offers high sensitivity and specific selectivity along with wide applicability and suitable of on-site applications. For instance, galvanic cell-based portable potentiometric sensors for soil moisture analysis [10] and self-chargeable electrochemical security sensor to detect and count intruders in a locality [11] have been reported recently. Additionally, significant progress has also been made using a wide variety of electrode modifier materials for the quantification and enhancement of the electrochemical performance in terms of selectivity, sensitivity and detection limit. For instance, graphene/carbon nanotubes and their composites have been extensively used owing to its outstanding electronic transport properties, high mechanical stability, large surface area, and high electrocatalytic activity [12–16]. The preparation of graphene from graphene oxide uses harsh chemicals and more importantly takes several days (almost one week). The conducting polymers and metal nanoparticles (mostly gold, platinum and silver) have been used to enhance the electron transfer [17–22] and thereby improve the sensitivity of the electrochemical sensors. Further, organic-based electrode materials have also been used for the selective quantification of heavy metal ions [23, 24]. However, the reported methods have the limitations of being expensive and require complex preparation methodologies and thereby not suitable for long-term storage and commercialization. Thus, it is of great interest to develop materials which are of low cost, environmentally benign and have specificity towards target analytes for the determination of Pb(II), Cd(II) and Hg(II) ions individually and simultaneously.

In this connection, Mn_3O_4 has attracted considerable interest owing to its outstanding electrocatalytic activity, great abundance of catalytic sites, high surface area and high stability. The potential applications of Mn_3O_4 has been extensively utilized in the field of lithium ion batteries, catalysis, and sensing of glucose and hydrogen peroxide [25–28], but Mn_3O_4 has not been, to the best of our knowledge, used for the detection of heavy metal ions to date.

The present investigation aims the fabrication of environmentally friendly electrode material with new qualities that can be exploited for analytical purpose with comparable or even better performance. In this paper, we develop Mns/graphitic carbon-based electrochemical sensors for the simultaneous quantification of Pb(II), Cd(II) and Hg(II) at nanomolar concentrations using differential pulse anodic stripping voltammetry (DPASV) for the first time. This novel material has been successfully prepared by simple and one-pot nitrate–sucrose decomposition methodology in less than 5 min (video, supporting information). Here, Mns provide highly active centres for the heavy metal ion accumulation and graphitic carbon provides necessary pathway for improving electron transport on modified electrode surface. The Mns/graphitic carbon sensors demonstrate excellent sensitivity with nanomolar levels possible using only a deposition time of 60 s. The Mns sensing tool is shown to be successfully applied and validated to the simultaneous determination of Pb(II), Cd(II) and Hg(II) in battery, industrial and chrome plating effluents at nanomolar levels.

Experimental section

Analytical grade manganese nitrate and sucrose were purchased from Sigma-Aldrich, and used without further purification. In a 100-mL borosil beaker, stoichiometric amounts of the manganese nitrate and sucrose [$Mn(NO_3)_2$/sucrose = 1:2] were dissolved in minimum quantity of double-distilled water. The homogeneous solution was directly introduced into the preheated muffle furnace which was maintained at 450 ± 10 °C. The solution first undergoes dehydration, thereby producing a viscous gel. This formed viscous gel starts to swell and occupies the whole beaker and then undergoes smouldering with the liberation of gaseous products, thereby forming ultralight and high surface area Mns/graphitic carbon. It is important to note that the overall synthetic procedure is fully completed in less than 5 min. It is worthwhile to mention that the reaction was

intentionally stopped at 5 min to retain graphitic carbon in the prepared Mns. This is a significant improvement over the current literature. The overall reaction for the formation of Mns can be expressed according to the following equation.

$$36Mn(NO_3)_{2(aq)} + 7C_{12}H_{22}O_{11(aq)} \rightarrow 12Mn_3O_{4(s)} + 36\ N_{2(g)} + 77H_2O_{(g)} + 84\ CO_{2(g)}$$

From the reaction, one can find that 16.4 mol of gases is liberated per one mole of Mn_3O_4 and the variation of crystallite size as a function of gaseous products liberated is summarized in Table S1 (supporting information).

Mn_3O_4 nanoparticle electrode fabrication

Glassy carbon electrode (3 mm diameter) was used as an electrode substrate. Prior to the electrode modification, the electrode surface was carefully polished with 1, 0.3 and 0.05 μm alumina powder to get a mirror surface. The polished electrode was washed with doubly distilled water followed by sonicated in doubly distilled water and absolute ethanol for 3 min to remove any adsorbed substances on the electrode surface, and finally dried in air. Five milligrams of Mns/graphitic carbon was dispersed into 5 mL distilled water via ultrasonication for 15 min to give a uniform suspension. Subsequently, the dispersed Mns/graphitic carbon suspension (0.006 mg) was drop-casted on the cleaned glassy carbon electrode surface and dried at room temperature. The unmodified GCE was prepared by the same procedure without using Mns/graphitic carbon.

Electrochemical performance measurements

All electrochemical measurements were carried out using CHI 619B electrochemical work station with a three-electrode system at room temperature. Mns/graphitic carbon, saturated Ag/AgCl and platinum electrode were used as working, reference and auxiliary electrode, respectively. All the solutions were degassed with high-purity nitrogen gas for 5–10 min before taking electrochemical measurements.

Electrochemical measurements of Pb(II), Cd(II) and Hg(II) were taken using differential pulse anodic stripping voltammetry between the potential range -1.1 and + 0.3 V with an amplitude of 0.01 V and pulse width of 0.05 s. Known amounts of analytes were placed into a 10-mL electrochemical cell, and the Mns/graphitic carbon sensor was immersed into the electrochemical cell containing a pH 5 acetate buffer solution and the target metal ions, which were stirred for 1 min to pre-concentrate the metal ions at open circuit. After this, the pre-concentrated metal ions were reduced at a reduction potential of − 1.1 V and subsequently stripped off from the Mns/graphitic carbon sensor surface into the bulk of the electrolytic solution by sweeping the potential in the positive direction after 30 s of equilibration time.

Characterization

The purity of the Mns/graphitic carbon has been monitored at room temperature using the powder X-ray diffraction (XRD) technique and Fourier transform infrared spectrometer (FTIR). The powder XRD measurements were performed using PANalytical X'pert PRO X-ray diffractometer with graphite monochromatized Cu Ka radiation source ($\lambda = 1.541$ A°). The FTIR spectrum of the sample was recorded at room temperature using Fourier transform infrared Nicolet spectrometer in the range 400–4000 cm^{-1}. BET surface area and nitrogen adsorption–desorption measurements were carried out at 77 K using a Quantachrome Corporation NOVA 1000. Transmission electron microscope (TEM) bright field images of the powder specimens were taken using a 300-keV field emission FEI Tecnai F-30 transmission electron microscope (TEM).

Results and discussion

Structural and morphological characterization of Mn_3O_4 nanoparticles

The purity, crystal structures and phase composition of the fabricated Mn_3O_4 nanoparticles as detailed in the experimental section were studied using powder XRD, the results of which are shown in Fig. 1a, where it is confirmed that all diffraction peaks are well indexed to a pure Mn_3O_4 with tetragonal structure (JCPDS 89-4837). It is important to note that no peaks of Mn_2O_3, MnO_2 and MnO are observed in the PXRD pattern, confirming the high purity. The average crystallite size (D) has been estimated using the Scherrer's formula, and it is found to be ~ 20 nm.

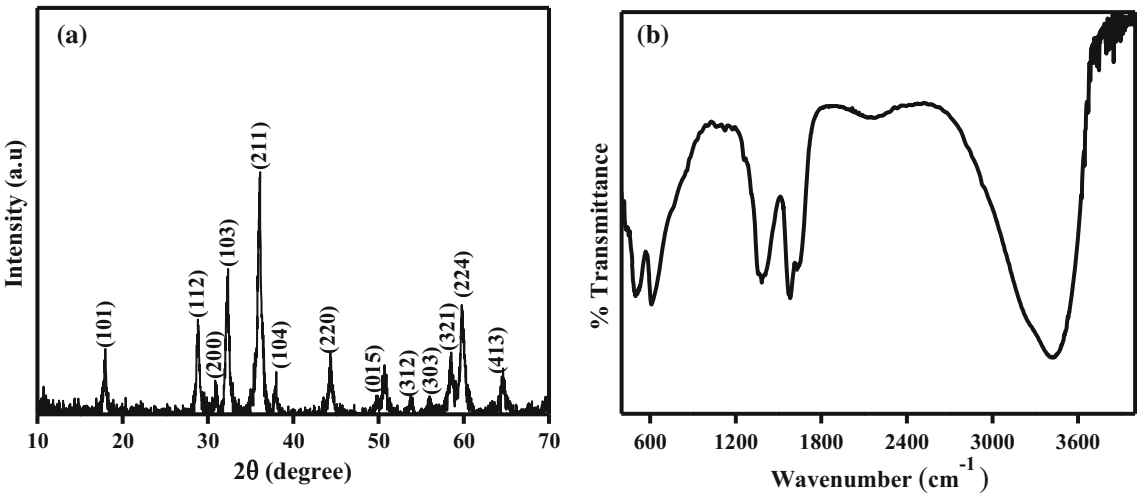

Figure 1 **a** Powder XRD pattern and **b** FTIR spectrum of the bespoke fabricated Mn_3O_4 nanoparticles.

(Details of crystallite size calculation are given in supporting information).

FTIR spectroscopy has been used to confirm the formation of Mn_3O_4 nanoparticles, as shown in Fig. 1b. Two absorption bands at 500 and 614 cm^{-1} appear in the FTIR spectrum and are associated with the coupling between Mn and O stretching mode of tetrahedral and octahedral sites [29]. The peaks at 1387 and 1580 cm^{-1} are due the presence of small amounts of carbon [30]. The peaks at 1387 and 1580 cm^{-1} are, respectively, assigned to the A_{1g} of disordered carbon and E_{2g} of graphitic carbon vibration modes. However, this observation has not been detected in the XRD data, which may be due to their very low quantity. Additionally, the broad bands at 3420, and 1634 cm^{-1} are attributed to O–H stretching and H_2O bending of physisorbed water, respectively.

BET surface area and N_2 adsorption–desorption measurements of Mns/graphitic carbon were also taken. The N_2 adsorption–desorption isotherm and pore size distribution of Mns/graphitic carbon are shown in Figure S1(a and b). The Mns/graphitic carbon exhibits type IV isotherm with H2 hysteresis type (Figure S1 a) according to the IUPAC classification. In the present synthesis methodology, as reported herein, the BET surface area of the Mns/graphitic carbon is found to be 66 $m^2\ g^{-1}$ and the pore size distribution obtained from desorption isotherms, shown in Figure S2 b, exhibits a narrow distribution centred at 29 nm. The obtained high surface area is due to the liberation of large amounts

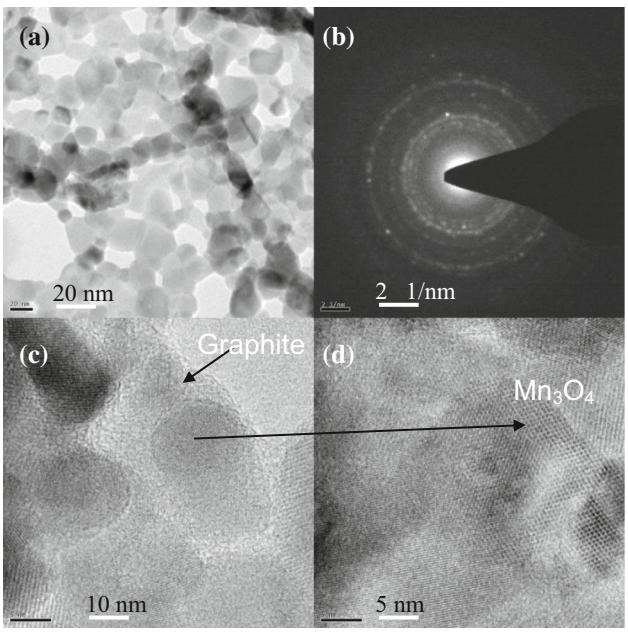

Figure 2 **a** TEM image, **b** SAED pattern and **c**, **d** HRTEM image of Mn_3O_4 nanoparticles.

of gaseous products such as carbon dioxide, nitrogen and water. The observed surface area is reasonably high as compared to the reported Mn_3O_4 (Table S2, supporting information).

TEM and high-resolution transmission electron microscopy have been carried out to study the microstructure of the prepared Mns/graphitic carbon. Figure 2a shows the typical low-magnification TEM image of the Mns/graphitic carbon. It clearly shows that the Mn_3O_4 exists in the form of

nanoparticles where the average particle size of the Mn_3O_4 is found to be ~ 20 nm which is consistent with the XRD results presented earlier. The nature of the Mn_3O_4 nanoparticles shown in Fig. 2b was further confirmed by SAED pattern. The clear visible diffraction rings can be indexed to the Hausmannite Mn_3O_4 phase. HRTEM images clearly provide the additional internal microstructure information of these Mn_3O_4 nanoparticles (Fig. 2c, d). The crystalline lattice fringes with interplanar spacing between the adjacent atomic lattice is 0.4932 nm, which is attributed to the tetragonal Mn_3O_4 and corresponds to the {101} plane. Additionally, it is interesting to note the presence of graphitic carbon along with the Mn_3O_4 nanoparticle (Fig. 2d). Thus, owing to its small crystallite size, large surface area and porous nature together with graphitic carbon, the prepared Mn_3O_4 nanoparticles have potential application in electrochemical sensors, where Mn_3O_4 nanoparticles provide active centres for metal ion accumulation and graphitic carbon can enable fast electron transport within electroanalysis [31].

Electrochemical characterization of Mn_3O_4/graphitic carbon

Furthermore, a comparative cyclic voltammetry study was performed on the bare and Mns/graphitic carbon GCE in acetate buffer (pH 5 and scan rate, 50 mVs^{-1}) over the potential range of -1.1 to +0.4 V in the absence and presence of 1 mM of Pb(II), Cd(II) and Hg(II) metal ions as shown within Fig. 3. The modified GCE does not showed any current signals for the oxidation of Mn_3O_4 to MnO_2 and/or the reduction of Mn_3O_4 to Mn^{2+} (aq). Hence, this could be used as an electrochemical interface for the measurement of Pb(II) Cd(II) and Hg(II) ions. The Mn_3O_4 nanoparticle-modified GCE (Fig. 3c) showed a significant signal/peak current at a peak potential of -0.75, -0.55 and $+0.2$ V owing to the oxidation potentials of Cd(II), Pb(II) and Hg(II) ions, respectively. Additionally, the reduction peak potentials were observed at -0.76, -0.48 and $+0.12$ V, respectively, for Cd(II), Pb(II) and Hg(II). The CV recorded using a bare glassy carbon electrode (Fig. 3b) showed a tiny peak current at a peak potential of $+0.12$ V under identical experimental conditions. This might be due to the oxidation of mercury present in the electrochemical cell. Furthermore, the Mns/graphitic carbon-modified electrodes

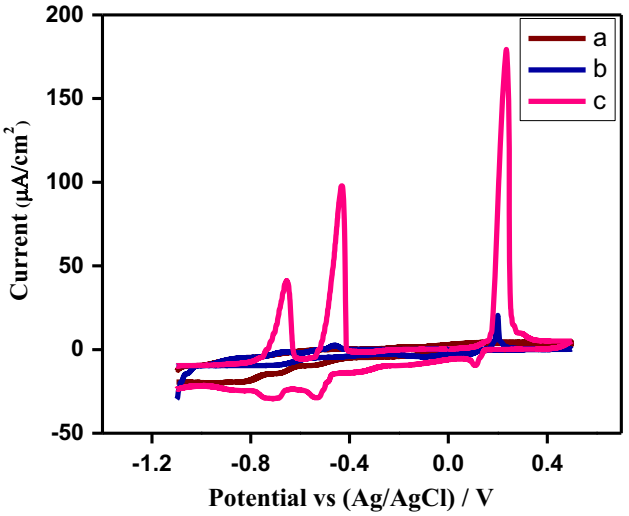

Figure 3 Overlaid cyclic voltammograms of the Mn_3O_4 nanoparticle sensor (*a*) in absence (*c*) in the presence of metal ions (*b*) bare (no Mn_3O_4 nanoparticles) glassy carbon electrode in the presence of 1 mM of Pb(II), Cd(II) and Hg(II) ions in buffer solution of pH 5 containing 0.1 M KCl as supporting electrolyte. Scan rate, 50 mV/s.

in the absence of the target metal ions (Fig. 3a) do not show any peak current in the same domain under identical experimental condition as well. This results presented above suggest that the Mns facilitates the improved electrochemical activity/performance due to its improvements in conductivity due to the presence of graphitic carbon favourable for enhancing the conductivity of the electrolyte [32] and mass transport changes due to the nanoparticle geometry. Additionally, the enhanced electrochemical activity might be attributed to a highly negative surface charge of manganese oxides [33, 34]. This negative surface charge increases the heavy metal ions adsorption capacity on Mn_3O_4. Hence, these studies reveal that the Mns/graphitic carbon-modified glassy carbon electrode can be used as electrochemical sensing platform for the detection of Pb(II), Cd(II) and Hg(II) within real sample matrices.

Based on CV results, the possible working mechanism of the proposed sensor is explained as follows. The obtained CV curve shows characteristic quasi-reversible behaviour. Here, the heavy metal ions are adsorbed on the electrode surface at open circuit potential. Subsequently, the reduction and oxidation take place at the electrode surface. Based on this, the following plausible working mechanism can be proposed [35].

(i) At open circuit potential

$$M^{2+}_{solution} + (\text{Modified GCE})_{surface} \rightarrow (\text{Modified GCE - } M^{2+})_{surface\ adsorption}$$

(ii) At applied potential

$$(\text{Modified GCE - } M^{2+})_{surface\ adsorption} + 2e \rightarrow (\text{Modified GCE - } M^{0})_{surface\ adsorption}$$

(iii) At stripping off

$$(\text{Modified GCE - } M^{0})_{surface\ adsorption} - 2e \rightarrow (\text{Modified GCE})_{surface\ adsorption} + M^{2+}_{solution}$$

Optimization of experimental parameters

In order to achieve the maximum efficiency of the modified electrode, various analytical parameters like pH, deposition potential, pre-concentration time and modifier volume were explored and consequently optimized using DPASV. The target analytes (0.5 μM) are pre-concentrated at the modified interface for 1 min by keeping the electrode in stirred solution and subsequently stripped off to the bulk of the electrolytic solution from the electrode surface by applying the sufficient negative potential by scanning the potential positive.

Effect of pH

The effect of pH on the DPASV response for Pb(II), Cd(II) and Hg(II) was investigated in the pH range of 2–9, and the results are shown in Fig. S2. As shown in Fig. S2, the peak current for all the target metal ions enhanced significantly up to pH 5 and then gradually reduced. The decrease in peak current with the increasing pH is due to the formation of metal hydroxides [36]. Therefore, pH 5 was chosen as an optimum pH for further detailed investigations.

Effect of deposition potential

The influence of the deposition potential upon the analytical signal/stripping signals was examined in the range − 0.1 to − 1.4 V (Fig. S3). It is observed that the peak current gradually increased from − 0.1 V to − 1.1 V and thereafter the sudden decrease for all the metal ions. Hence, the more negative the deposition potential will of course give rise to a larger analytical signal [37]; however, when the deposition potentials more negative than − 1.1 V were utilized, the stripping signals decrease due to the increased hydrogen evolution [38]. Hence, a deposition potential of − 1.1 V was chosen as an optimum potential for further experiments.

Effect of pre-concentration time

Fig. S4 shows the effect of accumulation time (30–180 s) upon the anodic stripping peak currents of Pb(II), Cd(II) and Hg(II) wherein the peak currents increased rapidly as the time increased from 30 to 60 s. After 60 s, the peak current decreased up to 180 s. The observed decrease in the current signal after 60 s is due to the saturation of active sites available on the electrode interface [39]. The observed high current signal for 60 s is very quick response resulting in a fast sensing protocol as compared to reported data [40–45] making this an advantageous material. Consequently, 60 s was chosen as the optimum accumulation time.

Effect of Mns/graphitic carbon mass coverage

The Mns/graphitic carbon suspension volume was drop-coated onto the electrode surface over the range 0.002–0.010 mg, and the results are presented in Fig. S5. The anodic peak current increases as the amount of material is increased from 0.002 to 0.006 mg. A further increase, up to 0.010 mg, decreases the analytical signal/peak current. The maximum signal/current is observed using 0.006 mg which is attributed due to more number of adsorption sites available on the modified electrode surface. In contrast, the decrease in peak current may be due to the saturation of the electrode surface. Therefore, Mns/graphitic carbon suspension volume of 0.006 mg has been chosen as an optimum mass.

Simultaneous determination of Pb(II), Cd(II) and Hg(II) using the Mn_3O_4 nanoparticle sensor

Under optimized conditions, to distinguish the electrocatalytic behaviour of the Mn_3O_4/graphitic carbon nanoparticle sensor towards the sensing of the target metal ions, the electrochemical sensing platform has

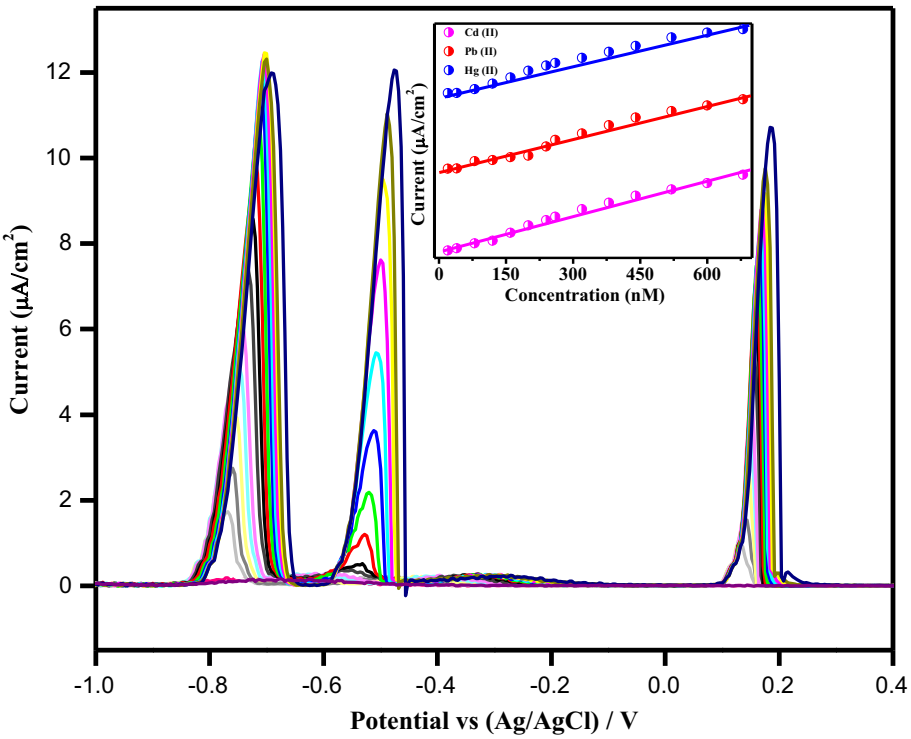

Figure 4 Overlaid anodic stripping voltammograms of Pb(II), Cd(II) and Hg(II) as a function of concentration range from 20 to 680 nM using the Mn_3O_4 nanoparticle electrode. Condition: deposition potential − 1.2 V, deposition time 60 s, potential scan range from − 1.0 to 0.4 V.

Table 1 Comparison of individual and simultaneous analysis of Pb(II), Cd(II) and Hg(II) using the Mn_3O_4 nanoparticle sensor

Analysis	Target metal ion	Deposition time	Linear equation	Correlation coefficient	Detection limit (3σ)
Individual	Cd(II)	60 s	I/μA = 0.02 (μA/nM)C + 1.23 (μA)	0.995	4.04×10^{-11} M
	Pb(II)		I/μA = 0.05 (μA/nM)C − 3.85 (μA)	0.996	3.40×10^{-11} M
	Hg(II)		I/μA = 0.04 (μA/nM)C + 15.73 (μA)	0.996	0.18×10^{-11} M
Simultaneous	Cd(II)		I/μA = 0.18 (μA/nM)C + 2.49 (μA)	0.996	0.48×10^{-11} M
	Pb(II)		I/μA = −0.01 (μA/nM)C + 1.23 (μA)	0.994	9.66×10^{-11} M
	Hg(II)		I/μA = −0.15 (μA/nM)C + 4.60 (μA)	0.995	0.51×10^{-11} M

been utilized for the determination of the target metal ions simultaneously and individually. Figure 4 shows the DPASV response of Pb(II), Cd(II) and Hg(II) over the concentration range 20–680 nM with corresponding calibration plots. Cd(II), Pb(II) and Hg(II) are, respectively, detected at peak potentials of − 0.76, − 0.6 and 0.2 V. As the concentration of the analyte increases, the peak current also increased proportionately, and the corresponding linear equation, correlation coefficient and limit of detection are given in Table 1. From inspection of Table 1, it is found that the limit of detection, based on 3-sigma, for Cd(II), Pb(II) and Hg(II) was found be 0.48×10^{-11}, 9.66×10^{-11} and 0.51×10^{-11} M, respectively. The observed limits of detections are clearly well within the threshold limits prescribed by WHO [4].

For completeness, the Mns/graphitic carbon sensor was used to quantify the target metal ions separately. The overlaid DPASV of Pb(II), Cd(II) and Hg(II) is shown in Fig. 5a–c. From Fig. 5a–c, it is observed that the peak current of Pb(II), Cd(II) and Hg(II) was proportionately increased as the concentration increases. The corresponding calibration plots are shown in Fig. 5d–f. The detection limit and

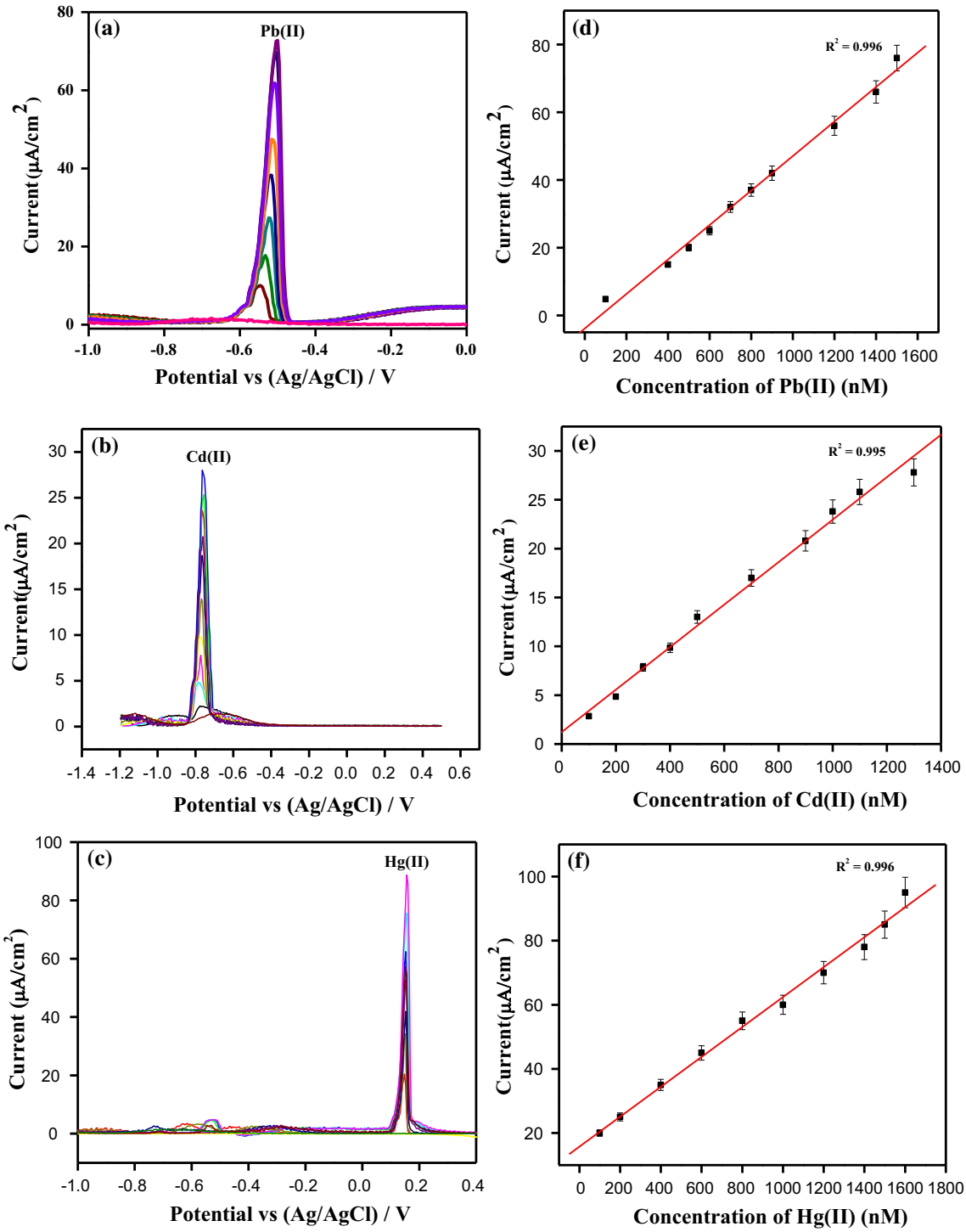

Figure 5 Overlaid differential pulse anodic stripping voltammograms of **a** Pb(II) in the concentration range 100–1500 nM using the Mn_3O_4 nanoparticle electrode, **b** Cd(II) in the concentration range 100–1500 nM **c** Hg(II) in the concentration range 100–1600 nM and **d**–**f** calibration plot of Pb(II), Cd(II) and Hg(II), respectively.

correlation coefficient of Pb(II), Cd(II) and Hg(II) are given in Table 1.

Interference study

The Mns/graphitic carbon sensor was examined in the presence of selected cations and anions which can potentially coexist in many real sample matrices. The possible mutual interferant species were added into the electrolytic solution containing the target analytes, and their impacts on the anodic peak currents were explored. The proposed interfacial results showed that in the presence of excess of other cations and anions, the signal deviations of 500 nM of Pb(II), Cd(II) and Hg(II) in the presence of other ions are not larger than 4%. Most of the cations and anions did not affect the simultaneous detection of Pb(II), Cd(II) and Hg(II) ions, when the optimized procedure was applied. 500-fold for Cl^-, F^-, SO_4^{2-}, K^+, Mn^{2+}, Li^+, Ag^+; 100-fold for Co^{2+}, $C_2O_4^{2-}$ and CO_3^{2-}; 20-fold for As^{3+}, Cr^{6+}, and F^-; 10-fold for Ni^{2+}, Fe^{2+} and Zn^{2+}. The relative standard deviations (RSD) of 7 measurements of 500 nM of Pb(II), Cd(II) and Hg(II) at modified electrode were 4.1, 3.5 and 4.8%, respectively.

Stability and repeatability of the proposed Mns/graphitic carbon sensor

The simultaneous measurement of Pb(II), Cd(II) and Hg(II) using the Mns/graphitic carbon sensor in the presence of 500 nM each of these ions was examined using the proposed protocol. The Mns/graphitic carbon sensor possesses good stability, retaining its performance characteristics over a period of 2 months and repeated usage with respect to their anodic stripping peak current. The life span of the Mns/graphitic carbon sensor was more than one month (30 determinations). The Mn_3O_4 nanoparticle sensor was kept in acetate buffer at pH 5 for a short period of time, and dry for a longer period of time. The electrochemical sensing tool exhibited good repeatability, with relative standard deviations of 3.58, 4.71 and 5.56% for Pb(II), Cd(II) and Hg(II) ions, respectively, for five successive runs. These experimental results revealed that the proposed Mns/graphitic carbon sensor can be used over a period of time and continuous analyses with precise analytical measurements. Hence, the Mns/graphitic carbon sensor can be used for the measurements of target

Table 2 Practical application study of the Mn_3O_4 nanoparticle sensor

Sample	Originally found (nM)			Added (nM)			Total found (nM)						Recovery (%)						RSD (%)		
							Proposed			ICP-OES			Proposed			ICP-OES					
	Pb^{2+}	Cd^{2+}	Hg^{2+}	Pb^{2+}	Cd^{2+}	Hg^{2+}	Pb^{2+}	Cd^{2+}	Hg^{2+}	Pb^{2+}	Cd^{2+}	Hg^{2+}	Pb^{2+}	Cd^{2+}	Hg^{2+}	Pb^{2+}	Cd^{2+}	Hg^{2+}			
Industrial effluents[a]	5.1	3.5	4.7	100	100	100	105.0	103.2	104.8	105.2	103.3	104.9	99.9	99.7	100.0	100.0	99.8	100.1	3.58		
Chrome plating industrial effluent[a]	ND	ND	3.5	100	100	100	99.9	100.1	103.1	100.3	101.1	103.0	99.9	101.1	99.6	103.3	101.1	99.5	4.71		
Battery effluent	8.7	11.1	ND	100	100	100	108.3	111.3	101.0	108.5	111.5	101.5	99.6	99.0	100.1	99.8	100.3	101.5	5.56		

ND not detected

[a]The samples were obtained from different open sewer lines within the city limits in the vicinity of industries

Table 3 Comparison of the Mn_3O_4-modified GCE performance with literature reports for the simultaneous detection of heavy metal ions

S. no.	Modified electrodes	Method	Metal ions	Deposition time (s)	Linear range	LOD	References
1	Mn_3O_4-GCE	DPASV	Pb(II)	60	20–680 nM	96.6 pM	Present
			Cd(II)		20–680 nM	48 pM	
			Hg(II)		20–680 nM	56 pM	
2	SnO_2/RGO	SWASV	Cd(II)	120	0.3–1.2 μM	0.104 nM	[40]
			Pb(II)		0.3–1.2 μM	0.184 nM	
			Cu(II)		0.3–1.2 μM	0.227 nM	
			Hg(II)		0.3–1.2 μM	0.279 nM	
3	Fe_3O_4	SWASV	Cd(II)	120	0.1–1.8 μM	0.213 μM	[41]
			Pb(II)		0.1–1.8 μM	0.06 μM	
			Cu(II)		0.1–1.8 μM	0.22 μM	
			Hg(II)		0.1–1.8 μM	0.059 μM	
4	AlOOH–RGO	SWASV	Cd(II)	120	0.2–0.8 μM	35 pM	[42]
			Pb(II)		0.2–0.8 μM	93 pM	
5	MgO/nafion	SWASV	Cd(II)	100	40–140 nM	81 pM	[43]
			Pb(II)		3.3–22 nM	2.1 pM	
6	NiO	SWASV	Cd(II)	120	0.1–1.2 μM	0.07 μM	[44]
			Pb(II)		0.1–1.2 μM	0.08 μM	
7	Bi_2O_3 SPE	SWSV	Cd(II)		10–150 μM	5 μM	[45]
			Pb(II)		10–150 μM	10 μM	

SNAC spherical carbon nanoparticle-decorated activated carbon, *GCE* glassy carbon electrode, *HAP* hydroxyapatite, *Ag NP-ZSM-5* silver nanoparticles decorated on ZSM-5 zeolite, *RGO* reduced graphene oxide, *PDMS* polydimethylsiloxane, *MWCNTs/NA* multi-walled carbon nanotube nanoarrays, *SPE* screen-printed electrode, *PPy* polypyrrole, *CNSs* carbonaceous nanospheres, *BONPs-IL-CPE* bismuth oxide nanoparticles and ionic liquid-modified carbon paste electrode, *SWSV* square wave stripping voltammetry, *SWASV* square wave anodic stripping voltammetry

metal ions at trace-level concentration, as regulated by WHO. Recoveries test was studied on a solution which contained different concentration ratios of metal ions.

Practical applications

In order to evaluate the proposed analytical method, the Mns/graphitic carbon sensor has been successfully applied for the quantification of Pb(II), Cd(II) and Hg(II) ions present in industrial, battery effluents and water samples. Industrial effluents and water samples were collected from different sources and filtered to remove any suspended particles. Five millilitres of real samples were diluted to 100 mL by adjusting the pH to 5, and 1 ml of this solution was added into the electrochemical cell containing the Mns/graphitic carbon sensor. The voltammetric stripping peak currents were measured and the concentrations determined using the standard addition protocol [46]. Known aliquots of standards were added to the real samples, and its recovery was also studied. The observed results were compiled in Table 2. From inspection of Table 2, it is observed that the recovery of HMIs was found to be in the range 99.6–101.5%, and the corresponding relative standard deviation was tabulated in Table 2. The performance of the proposed Mns/graphitic carbon sensor has been compared with the existing sensors (Table 3). The results reveal that the Mns/graphitic carbon sensor exhibits comparatively better analytical responses in terms of response time, LOD and wider linearity [40–45].

Conclusions

In summary, a new and excellent electroactive Mns/graphitic carbon electrode material has been developed and successfully utilized in the simultaneous determination of Pb(II), Cd(II) and Hg(II) at nM concentration by DPASV. The proposed modified electrode has an advantage of environmentally benign, ease of fabrication in large quantities, long-

term storage, and operational stability over a period of several months without loss of significant electrocatalytic activity and thereby suitable for on-site applications. Thus, the present study provides a new avenue for the fabrication of low cost electrochemical sensors using nanostructured metal oxides for heavy metal ion detection.

Acknowledgements

SA (Ashoka S) greatly thanks Science and Engineering Research Board (SERB, Project No. ECR/2017/000743) Government of India, for financial support to carry out this research work.

Electronic supplementary material: The online version of this article (https://doi.org/10.1007/s10853-017-1896-6) contains supplementary material, which is available to authorized users.

References

[1] Hua M, Zhang S, Pan B, Zhang W, Lv L, Zhang Q (2012) Heavy metal removal from water/wastewater by nanosized metal oxides: a review. J Hazard Mater 211–212:317–331

[2] Fu F, Wang Q (2011) Removal of heavy metal ions from wastewaters: a review. J Environ Manag 92:407–418

[3] Viyannalage LT, Bliznakov S, Dimitrov N (2008) Electrochemical method for quantitative determination of trace amounts of lead. Anal Chem 80:2042–2049

[4] World Health Organization (2011) World Health organization guidelines for drinking water quality, 4th edn. World Health Organization, Geneva, pp 389–395

[5] Li Y, Jiang Y, Yan XP, Peng WJ, Wu YY (2002) A flow injection on-line multiplexed sorption preconcentration procedure coupled with flame atomic absorption spectrometry for determination of trace lead in water, tea, and herb medicines. Anal Chem 74:1075–1080

[6] Ye QY, Li Y, Jiang Y, Yan XP (2003) Determination of Trace Cadmium in Rice by Flow Injection On-Line Filterless Precipitation–Dissolution Preconcentration Coupled with Flame Atomic Absorption Spectrometry. J Agric Food Chem 51:2111–2114

[7] Yaman M (2005) The improvement of sensitivity in lead and cadmium determinations using flame atomic absorption spectrometry. Anal Biochem 339:1–8

[8] Karami H, Mousavi MF, Yamini Y, Shamsipur M (2004) On-line preconcentration and simultaneous determination of heavy metal ions by inductively coupled plasma-atomic emission spectrometry. Anal Chim Acta 509:89–94

[9] Linge KL (2005) Recent developments in trace element analysis by ICP-AES and ICP-MS with particular reference to geological and environmental samples. Geostand Geoanal Res 29:7–22

[10] Pramod G, Mruthyunjayachari CD, Ravikumar T, Bhuneshwar P, Alagar RK, Harish MNK, Musthafa OT (2015) Galvanic cell type sensor for soil moisture analysis. Anal Chem 87:7439–7445

[11] Pramod G, Kavita K, Manasa N, Mruthyunjayachari CD, Shambhulinga A, Alagar RK, Zahid MB, Ravikumar T, Shahid PS, Musthafa OT (2017) Redox active binary logic gate circuit for homeland security. Anal Chem 89:7893–7899

[12] Mishra RK, Nawaz MH, Hayat A, Nawaz MAH, Sharma V, Martya JL (2017) Electrospinning of graphene-oxide onto screen printed electrodes for heavy metal biosensor. Sens Actuators B 247:366–373

[13] Pokhrela LR, Ettore N, Jacobs ZL, Zarr A, Weir MH, Scheuerman PR, Kanel SR, Dubey B (2017) Novel carbon nanotube (CNT)-based ultrasensitive sensors for trace mercury(II) detection in water: a review. Sci Total Environ 574:1379–1388

[14] Huang H, Chen T, Liu X, Ma H (2014) Ultrasensitive and simultaneous detection of heavy metal ions based on three-dimensional graphene-carbon nanotubes hybrid electrode materials. Anal Chim Acta 852:45–54

[15] Lee S, Oh J, Kim D, Piao Y (2016) A sensitive electrochemical sensor using an iron oxide/graphene composite for the simultaneous detection of heavy metal ions. Talanta 160:528–536

[16] Wang N, Lin M, Dai H, Ma H (2016) Functionalized gold nanoparticles/reduced graphene oxide nanocomposites for ultrasensitive electrochemical sensing of mercury ions based on thymine–mercury–thymine structure. Biosens Bioelectron 79:320–326

[17] Park MO, Noh HB, Park DS, Yoon JH, Shim YB (2017) Long-life heavy metal ions sensor based on graphene oxide-anchored conducting polymer. Electroanalysis 29:1521–4109

[18] Wang N, Dai H, Wang D, Ma H, Lin M (2017) Determination of copper ions using a phytic acid/polypyrrole nanowires modified glassy carbon electrode. Mater Sci Eng C 76:139–143

[19] Palanisamya S, Thangavelua K, Chen SM, Velusamy V, Chang MH, Chen TW, Al-Hemaid FMA, Ali MA (2017) Synthesis and characterization of polypyrrole decorated graphene/β-cyclodextrin composite for low level

electrochemical detection of mercury(II) in water. Sens Actuators B 243:888–894

[20] Suherman AL, Ngamchuea K, Tanner EEL, Sokolov SV, Holter J, Young NP, Compton RG (2017) Electrochemical detection of ultratrace (picomolar) levels of Hg2 + using a silver nanoparticle-modified glassy carbon electrode. Anal Chem 89:7166–7173

[21] Skotadis E, Tsekenis G, Chatzipetrou M, Patsiouras L (2017) Heavy metal ion detection using DNAzyme-modified platinum nanoparticle networks. Sens Actuators B 239:962–969

[22] de Barros A, Constantino CJL, da Cruz NC, Bortoleto JRR, Ferreira M (2017) High performance of electrochemical sensors based on LbL films of gold nanoparticles, polyaniline and sodium montmorillonite clay mineral for simultaneous detection of metal ions. Electrochim Acta 235:700–708

[23] Deshmukh S, Kandasamy G, Upadhyay RK, Bhattacharya G, Banerjee D, Maity D, Deshusses MA, Roy SS (2017) Terephthalic acid capped iron oxide nanoparticles for sensitive electrochemical detection of heavy metal ions in water. J Electroanal Chem 788:91–98

[24] Dai H, Wang N, Wang D, Ma H, Lin M (2016) An electrochemical sensor based on phytic acid functionalized polypyrrole/graphene oxide nanocomposites for simultaneous determination of Cd(II) and Pb(II). Chem Eng J 299:150–155

[25] Wang L, Wu KL, Jiang BB (2014) Non-enzymatic electrochemical sensors for the detection of H_2O_2 based on Mn_3O_4 octahedron submicrostructures. IET Micro Nano Lett 9:736–740

[26] Hao Q, Wang J, Xu C (2014) Facile preparation of Mn3O4 octahedra and their long-term cycle life as an anode material for Li-ion batteries. J Mater Chem A 2:87–93

[27] Li JJ, Li L, Wu F, Zhang L, Liu XM (2013) Dispersion–precipitation synthesis of nanorod Mn_3O_4 with high reducibility and the catalytic complete oxidation of air pollutants. Catal Commun 31:52–56

[28] Si P, Dong XC, Chen P, Kim DH (2013) A hierarchically structured composite of Mn_3O_4/3D graphene foam for flexible nonenzymatic biosensors. J Mater Chem B 1:110–115

[29] Dubal DP, Dhawale DS, Salunkhe RR, Lokhande CD (2010) A novel chemical synthesis of Mn_3O_4 thin film and its stepwise conversion into birnessite MnO_2 during super capacitive studies. J Electroanal Chem 647:60–65

[30] Zhu C, Sheng N, Akiyama T (2015) MnO nanoparticles embedded in a carbon matrix for a high performance Li ion battery anode. RSC Adv 5:21066–21073

[31] Li L, Guo Z, Du A, Liu H (2012) Rapid microwave-assisted synthesis of Mn_3O_4-graphene nanocomposite and its lithium storage properties. J Mater Chem 22:3600–3605

[32] Gu X, Yue J, Chen L, Liu S, Xu H, Yang J, Qian Y, Zhao X (2015) Coaxial MnO/N-doped carbon nanorods for advanced lithium-ion battery anodes. J Mater Chem A 3:1037–1041

[33] Murray J (1974) The surface chemistry of hydrous manganese dioxide. J Colloid Interface Sci 46:357–371

[34] Zou W, Han R, Chen Z, Jinghua Z, Shi J (2006) Kinetic study of adsorption of Cu (II) and Pb(II) from aqueous solutions using manganese oxide coated zeolite in batch mode. Colloids Surf A 279:238–246

[35] Nourifard F, Payehgadr M, Kalhor M, Nejadali A (2015) An electrochemical sensor for determination of Cd, Cu and Hg in water samples by modified carbon paste electrode base on a new Schiff base ligand. Electroanalysis 27:2479–2485

[36] Inczedy J (1976) Analytical applications of complex equilibria. Ellis Horwood, Halsted Press, New York

[37] Chaiyo S, Mehmeti E, Zagar K, Siangproh W, Chailapakul O, Kalcher K (2016) Electrochemical sensors for the simultaneous determination of zinc, cadmium and lead using a Nafion/ionic liquid/graphene composite modified screen-printed carbon electrode. Anal Chim Acta 918:26–34

[38] Yi H, Mei P (2008) Determination of cadmium (II) using H_2O_2-oxidized activated carbon modified electrode. J Appl Electrochem 38:1623–1627

[39] Morales GR, Silva TR, Galicia L (2003) Carbon paste electrodes electrochemically modified with cyclodextrins. J Solid State Electrochem 7:355–360

[40] Wei Y, Gao C, Meng FL, Li HH, Wang L, Liu JH, Huang XJ (2012) SnO2/reduced graphene oxide nanocomposite for the simultaneous electrochemical detection of cadmium(II), lead(II), copper(II), and mercury(II): An Interesting Favorable Mutual Interference. J Phys Chem C 116:1034–1041

[41] Li WJ, Yao XZ, Guo Z, Liu JH, Huang XJ (2015) Fe_3O_4 with novel nanoplate-stacked structure: surfactant-free hydrothermal synthesis and application in detection of heavy metal ions. J Electroanal Chem 749:75–82

[42] Gao C, Yu XY, Xu RX, Liu JH, Huang XJ (2012) AlOOH-reduced graphene oxide nanocomposites: one-pot hydrothermal synthesis and their enhanced electrochemical activity for heavy metal ions. ACS Appl Mater Interfaces 4:4672–4682

[43] Wei Y, Yang R, Yu XY, Wang L, Liu JH, Huang XJ (2012) Stripping voltammetry study of ultra-trace toxic metal ions on highly selectively adsorptive porous magnesium oxide nanoflowers. Analyst 137:2183–2191

[44] Li X, Wen H, Fu Q, Peng D, Yu J, Zhang Q, Huang X (2016) Morphology-dependent NiO modified glassy carbon electrode surface for lead(II) and cadmium(II) detection. Appl Surf Sci 363:7–12

[45] Kadara RO, Jenkinson N, Banks CE (2009) Disposable bismuth oxide screen printed electrodes for the high throughput screening of heavy metals. Electroanalysis 21:2410–2414

[46] Liu X, Li Z, Ding R, Ren B, Li Y (2016) A nanocarbon paste electrode modified with nitrogen doped grapheme for square wave anodic stripping voltammetric determination of trace lead and cadmium. Microchim Acta 183:709–714